Science Progress (2013), 96(3), 309–316
Doi:10.3184/003685013X13742175329073

Current Commentary

Novel catalysts for water splitting and green chemistry applications

CHRISTOPHER J. RHODES

Fresh-lands Environmental Actions, 88 Star Road, Caversham, Berks RG4 5BE, UK.
E-mail: cjrhodes@fresh-lands.com

1. Introduction

Catalysts enable molecular transformations to be carried out, while mitigating the inputs of thermal energy and other resources (in many cases solvents), and simultaneously curb the creation of residues that require later environmental disposal. A photocatalyst is a material that is able to harvest photons from light (ideally sunlight) and convert them to useful chemical energy, for which there are various "green" applications. Photocatalytic water splitting is the dissociation of water into its component elements, hydrogen and oxygen, to form H_2 and O_2, driven by the energy from light [Eqn (1)]. H_2 is one of the principally sought "solar fuels"[1], in which energy from sunlight might be stored, thus overcoming the issue of inconstant supply, which is an implicit limitation to renewable energy sources such as solar-power or wind-power.

Since water is a cheap and renewable resource, it appears very attractive as a solar fuel precursor, requiring only a suitable photocatalyst to accomplish the task. Capturing sunlight and converting it to chemical fuels is sometimes referred to as "artificial photosynthesis" (Figure 1). In principle, solar fuels might provide an alternative to the fossil fuels, serving the dual purpose of reducing carbon emissions and conserving declining fossil resources[2]: conventional crude oil production is expected to peak imminently, while the production of both[2] natural gas and coal is expected to peak around 2020. An independent analysis concludes that 90% of the world's reserves of coal will be used-up by the year 2070[3].

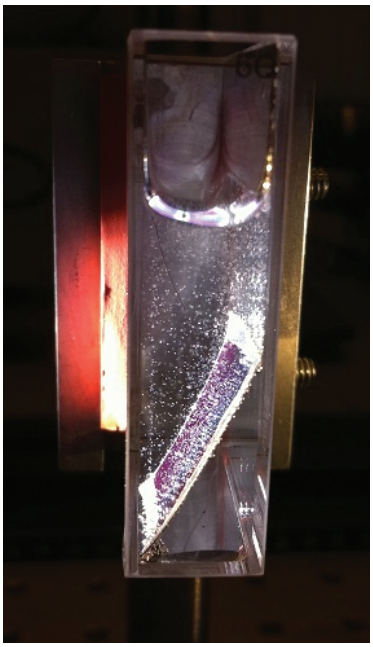

Figure 1 *"Artificial photosynthesis" in action. A sample of a photoelectric cell in a lab environment. Catalysts are added to the cell, which is submerged in water and illuminated by simulated sunlight. The bubbles seen are oxygen (forming on the front of the cell) and hydrogen (forming on the back of the cell).*
Credit: MisterRichValentine.
https://upload.wikimedia.org/wikipedia/commons/b/bc/Photo_Electric_Cell_Evolving_Hydrogen_and_Oxygen.jpg.

Water is most efficiently split using sunlight, on a semiconductor surface, Eqn (1).

$$2H_2O + h\nu \rightarrow 2H_2 + O_2 \quad (1)$$

An electric potential difference of at least 1.23 V is required to split water into hydrogen and oxygen. Typically, a cathodic overpotential of 100 mV and an anodic overpotential of 200 mV are also necessary, meaning that a band gap of at least 1.53 eV is required for splitting water[4,5]. As the band gap increases, the fraction of the solar spectrum the semiconductor can absorb decreases[6]. Appropriate energetic requirements must also be met, in terms of the valence and conduction band edges at the solution interface, since the energy bands must encompass the potentials at which the following half-reactions occur:

$$2H^+ + 2e^- \rightarrow H_2 \qquad -0.56 \text{ V } (vs \text{ Ag/AgCl}) \quad (2)$$

$$2H_2O \rightarrow O_2 + 4e^- + 4H^+ \qquad +0.67 \text{ V } (vs \text{ Ag/AgCl}) \quad (3)$$

In fact, the potentials associated with Eqns (2) and (3) will vary according to the Nernstian dependence on solution pH, and those values given above are for an electrolyte at pH = 6. Semiconductors in which the majority of charge carriers are electrons are classified as n-type, whereas those in which the majority of charge carriers are holes are designated as p-type[5]. The evolution of O_2 occurs on the surface of p-type materials while the evolution of H_2 occurs on the surface of n-type materials. To make a preliminary characterisation of semiconductors, open circuit potential measurements, photocurrent measurements, and Mott–Schottky analysis are applied[5]. The Fermi level of the material, which for n-type materials lies just below the conduction band, and for p-type materials lies slightly above the valence band, must be factored-in when estimating the location of the band edges[5].

Titanium dioxide (TiO_2) is one semiconductor which has an appropriate band structure to function as a photocatalyst for water splitting but, because of its relatively positive conduction band, the driving force for H_2 production is weak. The rate of H_2 production is enhanced when a co-catalyst such as Pt is introduced, and it is a common practice to add co-catalysts to accelerate H_2 evolution in photocatalytic systems, in consequence of the conduction band placement. The majority of those semiconductors that have suitable band structures for the splitting of water, tend to absorb light of UV wavelengths (< 400 nm). To permit the absorption of visible light, the band gap must be reduced. The conduction band is fairly close to the reference potential for H_2 formation and, in consequence, adjusting the valence band to bring it closer to the potential for O_2 formation is a better option, because there is a greater natural overpotential[4].

Under operating conditions, the disintegration of photocatalysts and electron-hole recombination are undesirable phenomena. Sulfide-based photocatalysts, *e.g.* CdS, are particularly sensitive because the sulfide component is oxidised to elemental sulfur at those same potentials that are employed to split water. To counteract this effect[4], sacrificial reagents are introduced, *e.g.* Na_2S. This replenishes the sulfur that is lost, and in essence, changes the principal reaction to one of hydrogen evolution, rather than water splitting. Recombination of the electron-hole pairs is a feature of many different types of catalyst and is influenced by the overall surface area of the catalyst and by defects that are present: recombination at the defect sites is impeded when there is a high degree of crystallinity present in the material[4].

2. Evaluation of the effectiveness of photocatalysts

Several crucial criteria must be met in order for a photocatalyst to be considered effective, one of which is that the H_2 and O_2 should be evolved in a stoichiometric 2:1 ratio. When the relative volumes of the two gases differ much from this, the indication is that the photocatalyst is not effective for water splitting. The quantum yield (QY) is the fundamental determinant of the catalyst efficiency, and is by definition[4]:

$$\text{QY (\%)} = (\text{Photochemical reaction rate}) / (\text{Photon absorption rate}) \times 100\%$$

To assist in comparing different photocatalysts, the rate of gas evolution can also be used, and while this measurement is more problematic when made in isolation, because it is not normalised, it is useful for a rough comparison and is routinely reported in the literature. The combined presence of a high quantum yield and a high rate of gas evolution may be taken to indicate an effective water-splitting photocatalyst. UV-based photocatalysts will be more effective *per photon absorbed* than those which employ visible light, as a result of a higher photon energy. However, since far more of the visible wavelengths are available at the Earth's surface than those in the UV range, a less effective catalyst but one which absorbs the visible part of the solar spectrum, may be more practically useful than one which absorbs in the UV[4].

3. Different types of photocatalyst

3.1 Pt/TiO_2

The most effective photocatalyst for water splitting is TiO_2, yielding a combined high quantum number and a rapid rate of H_2 gas evolution[4]. Co-particles consisting of the anatase form of TiO_2 and Pt form a photocatalyst that associates with a thin NaOH aqueous layer from which water is split into H_2 and O_2. As a result of its large band gap (>3.0 eV),TiO_2 absorbs principally in the UV region, but since it is relatively resistant to photo-corrosion, it is superior to the majority of photocatalysts that absorb visible light. Most ceramic materials are more strongly covalently bonded than other semiconductors, with accordingly larger band gap energies.

3.2 $NaTaO_3$:La

In the absence of sacrificial reagents, the greatest rate of photocatalytic water splitting is obtained using $NaTaO_3$:La[4]. This highly effective UV-based photocatalyst has demonstrated water splitting rates of 9.7 mmol h^{-1} with a quantum yield of 56%. The material possesses a nano-step structure, which is able to promote water splitting, in which the edges function as H_2 production sites and the grooves provide O_2 production sites. The H_2 production may be enhanced by the incorporation of a NiO co-catalyst. NiO has a lower conduction band than $NaTaO_3$ and hence photo-generated electrons are more easily transferred to the NiO conduction band to promote H_2 evolution[7].

3.3 $K_3Ta_3B_2O_{12}$

The catalyst[8], $K_3Ta_3B_2O_{12}$, absorbs only UV light, and has neither the performance nor quantum yield of $NaTaO_3$:La. Its advantage is that it can promote the splitting of water in the absence

of co-catalysts, at a quantum yield of 6.5%, and a water splitting rate of 1.21 mmol h^{-1}. This material has a pillared structure, consisting of TaO_6 pillars connected by triangular BO_3 units. No further enhancement was found when the catalyst was additionally loaded with NiO, in contrast with the behaviour[7] of $NaTaO_3$:La.

3.4 $(Ga_{0.82}Zn_{0.18})(N_{0.82}O_{0.18})$

Of those photocatalysts that absorb in the visible region of the solar spectrum, and which do not employ sacrificial reagents, $(Ga_{0.82}Zn_{0.18})(N_{0.82}O_{0.18})$ provides the greatest quantum yield – this being 5.9%, along with a water splitting rate of 0.4 mmol h^{-1} [4]. The properties of the catalyst may be adjusted by varying the temperature in the final calcination step. The number of surface Zn and O defects (which normally act as electron-hole recombination sites) was reduced by using temperatures up to 600 °C, albeit that temperatures above 700 °C were found to disrupt the local structure around the zinc atoms, with detrimental consequences for the effectiveness of the catalyst. An optimum performance of the catalyst was achieved[9] by additionally loading it with $Rh_{2-y}Cr_yO_3$ at a level of 2.5 wt% Rh and 2.0 wt% Cr.

4. Some recent developments in photocatalysts for hydrogen generation

Many cutting edge developments in the field of photocatalysis and related topics can be found in the journal "ACS Catalysis" (http://pubs.acs.org/journal/accacs), from which some of the following examples are taken.

Co-catalysts based on TiO_2 have been prepared containing both small platinum (Pt) nanoparticles and large gold (Au) particles, by employing a combination of traditional photodeposition of Pt in the presence of a hole scavenger (PH), with subsequent photodeposition of Au colloids, also in the presence of a hole scavenger. The Au particles had an average diameter of 13 nm and were attached to both TiO_2 and TiO_2-Pt samples. A strong photoabsorption in the region of 550 nm was observed for both the Au/TiO_2 and Au/TiO_2-Pt samples, resulting from the surface plasmon resonance (SPR) of Au. Naked TiO_2, TiO_2-Pt, Au/TiO_2, and Au/TiO_2-Pt samples were investigated for their ability to generate hydrogen (H_2) from aqueous solutions of 2-propanol by exposure to visible light. Only those samples containing Au particles were photoactive, and the rate of H_2 formation from the Au/TiO_2-Pt sample was larger by a factor of seven than that from the Pt-free Au/TiO_2 sample. This indicates that Pt nanoparticles loaded on TiO_2 form an effective cocatalyst, and provide reduction sites for H_2 evolution. From the series of cocatalysts prepared, of type M/TiO_2-Au, the H_2 evolution rates were found to decrease in the following order: Pt > Pd > Ru > Rh > Au > Ag > Cu > Ir.

From the linear correlation obtained between the H_2-evolution rate and the absorption of light, it may be inferred that SPR-induced photo-absorption by Au particles is a major factor in determining the rate of the H_2 evolution using these supported catalysts[10]. A method has been reported for generating unsupported nanopowders of Ni–Mo, which can be suspended in common solvents and cast onto various substrates. It was found that, in an alkaline environment, the mass-specific catalytic activity approached that of the best non-noble hydrogen evolution reaction (HER) catalysts, and the coatings have a good stability profile under the operating conditions. Turnover frequencies per surface atom were estimated at various overpotentials from which it is concluded that the increased activity of Ni–Mo over that for pure Ni is a result of combination of a greater surface area with a catalyst that is fundamentally more active[11].

To produce hydrogen from water, on a scale required to run the much heralded hydrogen economy, will necessitate appropriately sized electrolyser units. The efficiency of such devices can be increased by means of an effective catalyst, which lessens the amount of electricity required to split water into gaseous H_2 and O_2. Researchers at the University of Calgary say that they have developed a novel method for making catalysts using inexpensive metals (earth abundant elements), such as iron, cobalt, and nickel, as opposed to rare metals such as platinum, which are used in conventional catalysts for electrolysers.

More effective catalysts are necessary to reduce the kinetic barriers associated with the oxygen evolution reaction (OER). Most OER catalysts are based on crystalline mixed-metal oxides, but amorphous phases can also be highly active. Mixed-metal compositions are not, however, so readily obtained by existing methods. In contrast, a photochemical metal-organic deposition approach, can produce amorphous (mixed) metal oxide films for OER catalysis, which results in a homogeneous and accurately controllable distribution of metals. The catalytic properties of a-$Fe_{100-y-z}Co_yNi_zO_x$ are comparable to those of the current noble metal oxide catalysts employed in commercial electrolysers[12]. The spin-out company, FireWater Fuel intends to develop an electrolyser to produce hydrogen for energy storage at wind farms, and to create a commercial prototype for a freezer-size electrolyser that would convert a few litres of water a day to hydrogen for consumers by 2015[13]. The MIT spin-off company Sun Catalytix is working on a flow-battery intended for grid storage[14].

Flow batteries can be used to smooth out the variable supply of wind and solar farms or provide back-up power for buildings or campuses with on-site power generation. The principle of a flow battery is that there are two (large) tanks which contain an aqueous electrolyte, and these are pumped into a single tank with the two liquids held separate by a membrane. As the liquids are caused to flow in one direction into the "stack," an electrochemical reaction occurs across the membrane, generating an electric current. When the liquids are pumped in reverse, the device is recharged. It is intended that the Sun Catalytix flow battery could deliver one megawatt of power for four to six hours and fit in a 40-foot shipping container. The concept is well established, and there are dozens of commercial flow batteries connected to the grid which work on vanadium and zinc bromide systems. Using "abundant materials" it is hoped to get the price down to $200 to $250 per kilowatt-hour of storage capacity[14].

In a development of the "artificial leaf" concept[1,16] devised by Nocera, researchers at MIT have made an analysis with the aim to improve the efficiency of such systems, which they believe could enable the reality of a practical, inexpensive and commercially viable prototype[15]. This follows up on results published in 2011 that demonstrated proof of concept for an artificial leaf with the aim of producing hydrogen for remote installations, particularly in the non-legacy (developing) nations[16]. Although 4.7% or less of sunlight was converted into fuel using the original "leaf"[1,16], the new analysis indicates that greater efficiencies should be accessible using single-bandgap semiconductors, *e.g.* crystalline silicon (16%), or GaAs (18%)[15]. It has been reported in Chemistry World (September 2013, p13) that the "artificial leaf" is struggling to become a market reality, due both to technical challenges that must be overcome and uncertain returns on capital investment.

In connection with water-splitting and hydrogen fuel generation, researchers from the University of Oregon report[17] the solution synthesis, characterisation, and oxygen evolution reaction (OER) electrocatalytic properties of thin (2–3 nm) films of NiO_x, CoO_x, $Ni_yCo_{1-y}O_x$, $Ni_{0.9}Fe_{0.1}O_x$, IrO_x, MnO_x, and FeO_x. In alkaline media, the most active water-oxidation catalyst was found to be $Ni_{0.9}Fe_{0.1}O_x$ yielding 10 mA cm^{-2} at an overpotential of

336 mV with a Tafel slope of 30 mV dec^{-1}. Its OER activity was shown to be of an order of magnitude greater than the control IrO_x films, as is attributed to the *in situ* formation of layered $Ni_{0.9}Fe_{0.1}OOH$ oxyhydroxide species, in which practically all the Ni atoms are electrochemically active. It is concluded that these thin film catalysts may have applications, in conjunction with semiconductor photoelectrodes for direct solar-driven water splitting, or in the fabrication of high-surface-area electrodes for water electrolysis. A second paper from this group[18] details the performance of the catalyst thin films when combined with semiconductor light absorbers. A model is presented that describes the coupling of coloured OER electrocatalyst thin films with semiconductor photoelectrodes, from which is defined an "optocatalytic" efficiency (Φ_{o-c}) based on experimental optical and electrokinetic data measured under alkaline conditions. The most active catalyst was shown to be $Ni_{0.9}Fe_{0.1}O_x$, for which Φ_{o-c} is maximised (0.64) for a film thickness of ~0.4 nm (which amounts to two monolayers). It is concluded that such ultrathin films may provide the optimal working components of photocatalytic water splitting and electrolyser devices.

During the past two decades, new materials have been sought for oxygen evolution from catalytic water oxidation and for carbon dioxide reduction, with the aim of producing solar fuels. It is mostly inorganic materials that have been exploited and molecular complexes for water oxidation, in particular those inspired from our knowledge of how biological systems perform similar functions. A number of molecular water–oxidation complexes containing mono- or multinuclear catalytic sites have been investigated for their application to solution-phase generation of O_2. To undertake electro-catalytic or photo-electrochemical water oxidation, it is necessary to immobilise and functionalise the catalytic medium on an electrode surface, but there are a very limited number of examples where a molecular catalyst has been placed on a transparent conducting surface in such a system. A brief overview has been given[19] of surface-immobilised molecular assemblies for electrochemical water oxidation and recent progress in catalyst design and performance, including some systems-integrated modules that are envisaged in the fabrication of future stand-alone solar fuel generation devices.

5. Gratzel-type cells

While the focus of this current commentary is mainly on UV-absorbing electrodes, it would be an omission if at least some mention of multi-component dye-sensitised solar cells (DSSC) (Figure 2) were not made, *e.g.* of the Gratzel design[20,21], adaptations of which may be applied to water-splitting. Such cells typically contain TiO_2 and Pt electrodes, with a conducting electrolyte such as aqueous KI, of which many variants have been described, particularly with dye-sensitisation of the TiO_2 using *e.g.* Ruthenium complexes or organic dyes. Improvements in the efficiency of these devices have been achieved using nanocrystalline semiconductor forms[21], including quantum dot sensitisers[22].

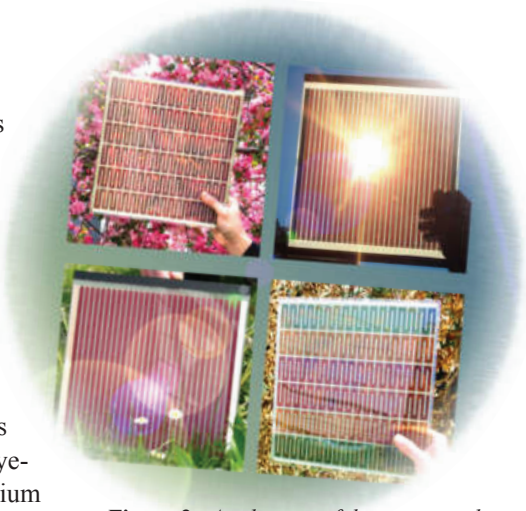

Figure 2 *A selection of dye-sensitised solar cells (DSSC).*
Credit: Sastra.
https://upload.wikimedia.org/wikipedia/commons/4/49/Dye.sensitized.solar.cells.jpg.

6. Other "green" catalytic applications

In addition to the development of catalysts for the splitting of water, and other means for the generation of solar fuels[1], are such catalysts as may enable the synthesis of organic compounds, in which the typical requirements of solvents, heating, and other inputs may be avoided or reduced, and as such may be designated as "green". A recent review has been made[23] of ring-expansion reactions of substrates bearing strained heterocyclic and carbocyclic rings published during the period 2006–2012. In some cases, enantiomerically enriched products are obtained by means of catalysts bearing primarily C-2 symmetric chiral organic motifs, and a diversity of metals are employed: Ti, Ni, Pd, Cu, Pt, Au, Rh, Fe, Ag, Al, Ru and In. Current models for the catalytic amination of methanol by zeolites are centred upon microporous shape-selective processes involving the molecules of monomethylamine (MMA), dimethylamine (DMA), and trimethylamine (TMA). In contrast, some additional aspects of shape-selective control are necessary to explain the uniquely high selectivity to MMA and DMA that pertains in Na^+-exchanged mordenite (Na^+-MOR). By means of modulation–excitation diffuse reflectance IR Fourier transform spectroscopy, with periodic perturbation by the isotope CD_3OD, it is shown that the H-bonded network of methanol agglomerates and open dimers in the micropores can readily be replaced by NH_3 at 623 K. It is thought that this may cause a decrease in the methanol concentration in the vicinity of catalytically active sites, hence resulting in a suppression of the consecutive reaction of MMA to DMA and, ultimately, to TMA[24]. It is known that he relative rates of the aldol reaction catalysed by supported primary and secondary amines can be inverted a hundred-fold, depending on the use of hexane or water as a solvent; in a recent study, it is shown that this dramatic shift in the catalytic behaviour of the supported amines does not involve differences in reaction mechanism, but is most likely caused by activation of imine to enamine equilibria and stabilisation of the iminium species. The effects of solvent polarity and acidity were found to be critical determinants of the reaction[25]. Cu-exchanged zeolites are widely used in catalytic convertors to suppress NO_x emissions from vehicles, and the ammonia-assisted selective catalytic reduction (NH_3-SCR) of NO_x is efficiently catalysed using Cu-exchanged chabazite (CHA framework). By means of multiple techniques, including crystallography and measurements of absorbed probe molecules, the active sites present have been fully characterised. Other zeolites with a high activity for NH_3–SCR include zeolites Y (FAU framework), ZSM-5 (MFI framework), SSZ-13 (CHA framework), and zeolite Beta (BEA framework). From the measurements reported[26], an accurate elucidation of the local geometry and environment of the Cu-based active sites within the zeolites can be described.

On the basis[27] of a combination of spectroscopic and catalytic investigations it has been inferred that, in the tungsten-catalysed H_2O_2 induced epoxidation of olefins, WO_3 (oxide) is the most active and stable phase rather than W(VI) species. It has further been discovered that a nanoparticulate WO_3 prepared by flame aerosol technology gives an optimum performance, and is characterised by a 50% increase in activity per W(VI) site, and a 35-fold increase in space time yield, over the currently employed benchmark catalyst. The biocatalytic potential of "-ene" reductases from the old yellow enzyme (OYE) family of oxidoreductases is well-known, and provides a means to the production of various high-value chemicals. In order to broaden the potential industrial perspective of the approach, a flavin-free double bond reductase from *Nicotiana tabacum* (NtDBR), which belongs to the leukotriene B_4 dehydrogenase (LTD) subfamily of the zinc-independent, medium chain dehydrogenase/reductase superfamily of enzymes, has been characterised. In addition to catalysing the reduction of typical LTD substrates and several classical OYE-like substrates, NtDBR was found also to exert a

complementary activity by reducing non-OYE substrates (*i.e*. reducing the exocyclic C=C double bond of (*R*)-pulegone) and in some cases an opposite stereo-preference was obtained, in comparison with the OYE family member, pentaerythritol tetranitrate (PETN) reductase[28].

References.

1. Rhodes C.J. (2012) *Sci. Prog*., **95**, 206.
2. http://www.energywatchgroup.org/fileadmin/global/pdf/EWG-update2013_long_18_03_2013.pdf.
3. Rutledge, D. (2011) *Int. J. Coal Geol*., **85**, 23.
4. Kudo, A. and Miseki, Y. (2009) *Chem. Soc. Rev*., **38**, 253.
5. Head, J. and Turner, J. (2001) *U.S. Department of Energy Journal of Undergraduate Research*, January 2001. http://www.osti.gov/bridge/servlets/purl/1051819/1051819.pdf.
6. Rhodes, C.J. (2010) *Sci. Prog*., **93**, 37.
7. Kato, H., Asakura, K. and Kudo, A. (2003) *J. Am. Chem. Soc.*, **125**, 3082.
8. Kurihara, T. *et al.* (2006) *Chem. Lett*., **35**, 274.
9. Maeda, K., Teramura, K. and Domen, K. (2008) *J. Catal*., ***254,*** 198.
10. Tanaka, A. *et al.* (2013) *ACS Catal.,* **3**, 79.
11. McKone, J.R. *et al.* (2013) *ACS Catal.,* **3**, 166.
12. Smith, R.D.L. *et al*. (2013) *Science*, **340**, 60.
13. http://www.technologyreview.com/view/512996/a-cheaper-way-to-make-hydrogen-from-water/
14. http://www.technologyreview.com/view/512071/sun-catalytix-seeks-second-act-with-flow-battery/
15. Winkler, M.T. *et al*. (2011) *Proc. Nat. Acad. Sci*., **110**, E1076. http://www.pnas.org/content/110/12/E1076.
16. Reece, S.Y. *et al*. (2011) *Science,* **334**, 645.
17. Trotochaud, L. *et al*. (2012) *J. Am. Chem. Soc.,* **134**, 17253.
18. Trotochaud, L., Nills, T.J. and Boettcher, S.W. (2013) *J. Phys. Chem. Lett*., **4**, 931.
19. Joya, K.S. *et al*. (2013) *ChemPlusChem*., **78**, 35.
20. Xiong, D. and Chen, W. (2012) *Front. Optoelectron,* 5, 371.
21. Gratzel, M. (2001) *Nature,* **414**, 338.
22. Shin, K. *et al* (2013) *J. Power Sources*, **225**, 263.
23. Mack, D.J. and Njardarson, J.T. (2013) *ACS Catal.*, **2**, 272.
24. Maeda, N. *et al.* (2013) *ACS Catal.,* **3**, 219.
25. Kandel, K. *et al*. (2013) *ACS Catal.,* **3**, 265.
26. Deka, U. *et al.* (2013)*, ACS Catal.,* **3**, 413.
27. Hammond, C. *et al*. (2013) *ACS Catal.,* **3**, 321.
28. Mansell, D.J. *et al*. (2013) *ACS Catal.,* **3**, 70.